Research Article

Haleema Ali, Rasool Khan*, Xiandao Pan, Farzana Shaheen, Almas Jabeen, Abdur Rauf*, Muhammad Shah, Umer Rashid, Yahya S. Al-Awthan, Omar S. Bahattab, Mohammed A. Al-Duais, and Mohammad S. Mubarak

Synthesis, characterization, anticancer, anti-inflammatory activities, and docking studies of 3,5-disubstituted thiadiazine-2-thiones

https://doi.org/10.1515/gps-2022-8136
received November 09, 2022; accepted February 12, 2023

Abstract: In the search for potent bioactive compounds, a series of tetrahydro-2*H*-1,3,5-thiadiazine-2-thiones (**1**–**13**) were synthesized in good yield and characterized by means of ^{1}H NMR, ^{13}C NMR, and mass spectral data. The anticancer activity of the compounds was evaluated against HeLa cell line and anti-inflammatory potential via nitric oxide (NO) inhibition. Among the screened compounds, 2-(5-(3-methoxypropyl)-6-thioxo-1,3,5-thiadiazinan-3-yl) propionic acid (**3**), 2-(5-cyclopropyl-6-thioxo-1,3,5-thiadiazinan-3-yl) propionic acid (**5**), 2-(5-cyclopropyl)-6-thioxo-1,3,5-thiadiazinan-3-yl) acetic acid (**6**), and 2-(5-butyl-6-thioxo-1,3,5-thiadiazinan-3-yl) acetic acid (**9**) were the most potent against HeLa cell line with IC_{50} values <4 μM, whereas the rest of the series exhibited moderate-to-good activities. All the compounds were potent NO inhibitors with IC_{50} values ranging from <0.4 to 14.9 μM. Docking studies, binding orientations, and interaction plots showed strong interaction of the studied compounds with the inducible NO synthase enzyme via strong hydrogen bonds and hydrophobic interactions, which authenticate the in vitro results. These newly synthesized compounds could lead to the discovery of anticancer drugs.

Keywords: thiadiazine thione, inducible nitric oxide synthase, HeLa cell line, docking studies

*** Corresponding author: Rasool Khan,** Institute of Chemical Sciences, University of Peshawar, Peshawar-25120, Khyber Pakhtunkhwa, Pakistan, e-mail: rasoolkhan1@hotmail.com
*** Corresponding author: Abdur Rauf,** Department of Chemistry University of Swabi, Swabi, Anbar, 23561, Khyber Pakhtunkhwa, Pakistan, e-mail: mashaljcs@yahoo.com
Haleema Ali: Institute of Chemical Sciences, University of Peshawar, Peshawar-25120, Khyber Pakhtunkhwa, Pakistan
Xiandao Pan: Beijing Key Laboratory of Active Substance Discovery and Drug Ability Evaluation Institute of Material Medical, Chinese Academy of Medical Sciences and Peking Union Medical College, Beijing, China
Farzana Shaheen: HEJ Research Institute of Chemistry, International Canter for Chemical and Biological Sciences (ICCBS), University of Karachi, Karachi 75270, Pakistan
Almas Jabeen: Dr. Panjwani Center for Molecular Medicine and Drug Research, International Center for Chemical and Biological Sciences (ICCBS), University of Karachi, Karachi, 75270, Pakistan
Muhammad Shah, Umer Rashid: Department of Chemistry, COMSATS University Islamabad, Abbottabad Campus, 22060 Abbottabad, Pakistan
Yahya S. Al-Awthan: Department of Biology, Faculty of Science, University of Tabuk, Tabuk 71421, Saudi Arabia; Department of Biology, Faculty of Science, Ibb University, Ibb 70270, Yemen
Omar S. Bahattab: Department of Biology, Faculty of Science, University of Tabuk, Tabuk 71421, Saudi Arabia
Mohammed A. Al-Duais: Department of Biochemistry, Faculty of Science, University of Tabuk, Tabuk 71421, Saudi Arabia; Chemistry Department, Biochemistry Unit, Faculty of Science, Ibb University, Ibb 70270, Yemen
Mohammad S. Mubarak: Department of Chemistry, The University of Jordan, Amman 11942, Jordan

1 Introduction

The recent call of World Health Organization for the elimination of cervical cancer as a global health concern prompted medicinal chemists to search and develop potent molecules for treating cancer [1]. Cervical cancer is the fourth most common cancer in women, and the leading cause of death in low-resource countries [2]. According to recent research in chemotherapy, there is a pressing need for more compelling anticancer mediators since the effectiveness of chemotherapy is limited by tumor cells' heterogeneity and drug resistance [3,4]. Nitric oxide (NO) is a liposoluble molecule, endogenously produced in the mammalian body during the metabolism of L-arginine to L-citrulline by the action of nitric oxide synthases (NOS) [5]. NO is a versatile intra- and intercellular

messenger controlling diverse pathophysiological mechanisms in circulatory, neurological, and immune systems [6]. Despite biological mediators, NO, as an oxygen free radical, is cytotoxic in pathological processes, mainly in inflammatory ailments [7]. Furthermore, inflammation should be regulated because of its direct impact on chronic conditions, such as cancer, cardiovascular, and immunological diseases [8]. Thus, inflammatory diseases can be treated by NO inhibition [9].

Currently, NO is recognized as one of the most important molecules affecting the growth, development, and treatment of cancer. In tumor biology, NO has both positive and negative effects, as it has been associated with both endorsing and inhibiting cancer. Research findings indicated that the dual responses of NO toward cancer are due to its concentration-dependent ability in development, migration, incursion, persistence, and metastasis of tumor [10]. The exact molecular mechanism of NO involvement in cancer is not fully understood so far; however, studies found a significantly higher levels of NO in cervical cancer patients [11]. In addition, cervixes of women having cervical intraepithelial neoplasia were found with elevated levels of NO as well as NO-mediated mutagenesis [12]. These studies concluded mutagenic and carcinogenic activities of NO in cervical cancer.

Synthesis of novel molecules possessing pharmacophore moiety that resembles known biologically active compounds provides a leading approach toward the development of highly active agents. Among anticancer agents, dithiocarbamates [13–17] and isothiocyanate [18–24] gained great attention as promising anticancer candidates. In addition, tetrahydro-(*2H*)-1,3,5-thiadiazine-2-thione nucleus has been reported to exhibit anticancer [25–29], antileishmanial [30], antibacterial [31], trypanocidal [32], antimalarial [33], antifungal [34], herbicidal [35], antitubercular [36], antiepileptic [37], and antioxidant [38] activities. These activities were attributed to the formation of isothiocyanate and dithiocarbamic acid upon hydrolysis of this nucleus in biological systems [29,39].

On the basis of the previous discussion, the aim of the present work was to synthesize 3,5-disubstituted thiadiazine-2-thiones as potential anticancer agents. The anticancer activity of the synthesized compounds will be evaluated against human cervical cancer HeLa cell line. Previously, the anticancer activity of cyclopentyl, cyclohexyl, and furfuryl N-3 substituted and *bis*-disubstituted thiadiazine-2-thiones has been tested against HT-29 (Human colorectal adenocarcinoma), A549 (lung carcinoma), Hep3B (hepatocellular carcinoma), HepG2 (hepatocellular carcinoma), U-87MG (Brain (glioblastoma astrocytoma), normal cell line (fibroblast F180) [25], K562 (leukaemia cells), MCF12 (normal cells) [26], MCF-12A (normal breast cell line), MCF-7 and MDA-MB-468 (breast cancer cell line) [27], Hep G2 (human hepatoma), HT-29 (human colon carcinoma), and HeLa (human cervical carcinoma) [28,29]. These studies showed moderate-to-good activity of the tested derivatives of tetrahydro-2*H*-1,3,5-thiadiazine-2-thione. We, therefore, sought to synthesize more functionalized tetrahydro-2*H*-1,3,5-thiadiazine-2-thiones, which could be more potent than previously reported ones. Despite the wealth of literature that dealt with the biological properties of 1,3,5-thiadiazine-2-thione moiety, no anti-inflammatory activity has been assessed for this nucleus. Hence, this study deals with the anticancer and NO inhibitory potential along with the docking studies of the titled compounds to appraise the functional modification on the 1,3,5-thiadiazine-2-thione nucleus for the said activities.

2 Materials and methods

2.1 Chemistry

All chemicals and reagents were obtained from commercial suppliers and used as received without further purification. Reactions were monitored by thin-layer chromatography, achieved on silica gel plates (60 F-254); these plates were visualized under UV light. Melting points were determined using a Gallen Kamp melting point apparatus and are uncorrected. Dimethyl sulfoxide (DMSO), chloroform ($CDCl_3$), and methanol (CD_3OD) were used as solvents for NMR Spectra. ^1H and ^{13}C NMR spectra were recorded on Bruker AVNeo-NMR Spectrometers and using TMS as an internal standard. Chemical shifts are expressed in δ units, whereas coupling constants (*J*-values) are given in Hertz. Mass spectra were acquired on JEOL MS Route and Finnigan LTQ FTMS (ESI) spectrometer.

2.2 General procedure for synthesis of 3,5-disubstituted tetrahydrothiadiazine-2-thiones (1–13)

Compounds **1**–**13** were prepared by adding selected alkyl/cycloalkyl/aryl amine (20 mmol) to a 20% KOH aqueous solution followed by adding CS_2 dropwise (20 mmol) at 30°C with stirring. After 4 h, 37% formaldehyde solution (40 mmol) was added and stirred for 1 h continuously, and the reaction mixture was then filtered and added, dropwise, to a suspension of amino acid or primary amines

(20 mmol) in a 7.8 pH phosphate buffer and stirred for 1 h (Scheme 1). The mixture was then filtered and refrigerated for 1 h. The ice-chilled reaction mixture was acidified with hydrochloric acid up to pH 2.0 at 0–5°C. The precipitate formed was thoroughly washed with water followed by *n*-hexane and then dried. The desired product was recrystallized from ethanol to afford pure compounds **1**–**13**. Using this general procedure, the following compounds were synthesized.

2.2.1 2-(5-butyl-6-thioxo-1,3,5-thiadiazinan-3-yl)-4-methylpentanoic acid (1)

Compound **1**, acquired by *n*-butyl amine and L-leucine, was obtained as white solid recrystallized from ethanol. Yield: 76%, mp: 92–94°C. ^{1}H NMR (600 MHz, DMSO-d_6): δ 0.89 (t, 9H, J = 6.4, CH_3), 1.25–1.31 (m, 2H, $CH_3CH_2CH_2$), 1.50–1.63 (m, 5H, $CH_2CH_2CH_2$, CH_3CHCH_3, $CHCH_2CH$), 3.50–3.53 and 3.79–3.98 (m, 2H, NCH_2CH_2,), 4.45–4.64 (m, 4H, NCH_2NCH_2S), ^{13}C NMR (150 MHz, DMSO-d_6): δ 13.87 (CH_3CH_2), 19.69 (CH_3CH_2), 21.93, 23.43 (CH_3CHCH_3), 24.96 (CH_3CHCH_3), 28.37 ($CH_2CH_2CH_2$), 38.67 ($CHCH_2CH$), 51.48 (NCH_2), 55.75 (C-6), 60.77 (NCH), 67.61 (C-4), 173.46 (CO), 190.58 (CS). MS (70 eV): m/z (%): m/z (%) = 304.2 (4.5) $[M]^+$, 256.2 (11) $[M-146]^+$, 140.0 (100) $[M-200]^+$, 115.1 (100) $[M-289]^+$.

2.2.2 2-(5-butyl-6-thioxo-1,3,5-thiadiazinan-3-yl) butanoic acid (2)

Compound **2** was obtained from *n*-butyl amine and *DL*-2-aminobutyric acid as a white solid recrystallized from ethanol. Yield: 72%, mp: 93–95°C (600 MHz, DMSO-d_6): δ 0.84–0.91 (m, 6H, CH_3CH_2, CH_3CH_2), 1.23–1, mp: 32 (m, 2H, $CH_3CH_2CH_2$), 1.50–1.61 (m, 2H, $CH_2CH_2CH_2$) 1.70–1.84 (m CH_3CH_2CH), 3.40–3.43 (m 1H, NCH), 3.69–3.76 and 4.02–4.09 (m, 2H, NCH_2CH_2,), 4.44–4.51 (m, 2H, NCH_2S), 4.59–4.64 (m, 2H NCH_2N), ^{13}C NMR (150 MHz, DMSO-d_6): δ 9.28 (CH_3CH_2CH), 13.57 ($CH_3CH_2CH_2$), 19.36 ($CH_3CH_2CH_2$), 22.31 ($CHCH_2CH$), 28.00 ($CH_2CH_2CH_2$), 51.10 (NCH_2), 55.45 (C-6), 61.74 (NCH), 67.44 (C-4), 172.50 (CO), 190.39 (CS). MS (70 eV): m/z (%) = 276.2 (10) $[M]^+$, 246.2 (25) $[M-30]^+$, 128.0 (45) $[M-148]^+$, 115.0 (100) $[M-161]^+$.

2.2.3 2-(5-(3-methoxypropyl)-6-thioxo-1,3,5-thiadiazinan-3-yl) propionic acid (3)

Compound **3** was synthesized from 3-methoxyropyl amine and β-alanine and obtained as a white solid. Yield: 72%, mp: 98–100°C. ^{1}H NMR (400 MHz, MeOD): δ 1.96–2.02 (m, 2H, $CH_2CH_2CH_2$), 2.58 (t, 2H, J = 8, NCH_2CH_2), 3.10 (t, 2H, J = 8, CH_2CH_2COOH), 3.34 (s, 3H, CH_3O), 3.47 (t, 3H, J = 8, OCH_2CH_2), 4.07 (t, 2H, J = 8, NCH_2CH_2), 4.49 (s, 2H, NCH_2S), 4.50 (s, 2H, NCH_2N). ^{13}C NMR (100 MHz, MeOD): δ 28.10 ($CH_2CH_2CH_2$), 34.26 (CH_2COOH), 47.63 (NCH), 51.10 (NCH_2), 59.04 (CH_3O), 59.14 (C-6), 71.22 (OCH_2), 71.82 (C-4), 175.90 (CO), 193.72 (CS). High-resolution mass spectrometry (HRMS) (ESI) m/z: calculated for $C_{10}H_{19}N_2O_3S_2$ $[M+H]^+$ 279.08371; found 279.08344.

2.2.4 2-(5-(3-methoxypropyl)-6-thioxo-1,3,5-thiadiazinan-3-yl) acetic acid (4)

Compound **4** was acquired by 3-methoxyropyl amine and glycine. Product obtained as white solid. Yield: 71%, mp: 101–103°C. ^{1}H NMR (400 MHz, DMSO-d_6): δ 1.79–1.86

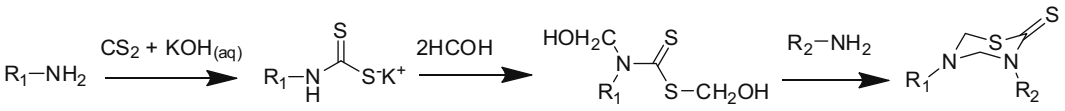

R1=

-C_4H_9 **1,2,7,9**

-C_4H_9O **3,4**

-C_3H_5 **5,6**

-C_3H_7 **8**

-C_6H_5- **10,11,12,13**

R2=

-$C_6H_{11}O_2$ **1,13**

-$C_4H_7O_2$ **2**

-$C_3H_5O_2$ **3,5,7,12**

-$C_2H_3O_2$ **4,6,8,9**

Scheme 1: General scheme for the synthesis of the title compounds.

(m, 2H, $CH_2CH_2CH_2$), 3.22 (s, 2H, NCH_2COOH) 3.34 (t, 2H, J = 8, NCH_2CH_2), 3.53 (s, 3H, CH_3O), 3.93 (t, 3H, J = 8, OCH_2CH_2), 4.51 (s, 2H, NCH_2S), 4.52 (s, 2H, NCH_2N). ^{13}C NMR (100 MHz, DMSO-d_6): δ 35.63 ($CH_2CH_2CH_2$), 58.50 (NCH), 60.16 (NCH2), 67.31 (CH_3O), 67.48 (C-6), 78.77 (OCH_2), 79.24 (C-4), 180.04 (CO), 199.69 (CS). HRMS (ESI) m/z: calculated for $C_9H_{17}N_2O_3S_2$ $[M+H]^+$ 265.06806; found 265.06744.

2.2.5 2-(5-cyclopropyl-6-thioxo-1,3,5-thiadiazinan-3-yl) propionic acid (5)

Compound **5** was acquired by cyclopropyl amine and DL-α-alanine. Product obtained as white solid. Yield: 69%, mp: 123–124°C. ^1H NMR (400 MHz, DMSO-d_6): δ 0.78–0.90 (m, 4H, cyclopropyl ring protons), 2.50 (m, 3H, CH_3CH), 2.88 (t, 1H, J = 8, CH_3CH), 3.07–3.13 (m, 1H, NCH), 4.40 (s, 2H, NCH_2S), 4.41 (s, 2H, NCH_2N), 12.22 (s, COOH). ^{13}C NMR (100 MHz, DMSO-d_6): δ 7.66 (cyclopropyl ring carbons), 32.29 (CH_3CH), 35.06 (NCH), 45.14 (C-6) 56.19 (NCH), 70.22 (C-4), 172.65 (CO), 192.84 (CS). HRMS (ESI) m/z: calculated for $C_9H_{15}N_2O_2S_2$ $[M+H]^+$ 247.05749; found 247.05711.

2.2.6 2-(5-cyclopropyl)-6-thioxo-1,3,5-thiadiazinan-3-yl) acetic acid (6)

Compound **6** was acquired by cyclopropyl amine and glycine. Product obtained as white solid. Yield: 72%, mp: 122–124°C. ^1H NMR (400 MHz, DMSO-d_6): δ 0.74–0.88 (m, 4H, cyclopropyl ring protons), 3.04–3.09 (m, 1H, NCH), 3.49 (s, 2H, NCH_2COOH), 4.42 (s, 2H, NCH_2S), 4.46 (s, 2H, NCH_2N), 12.65 (s, COOH). ^{13}C NMR (100 MHz, DMSO-d_6): δ 8.10 (cyclopropyl ring carbons), 35.31 (NCH), 50.63 (NCH2), 57.10 (C-6), 70.44 (C-4), 170.69 (CO), 193.32 (CS). HRMS (ESI) m/z: calculated for $C_8H_{13}N_2O_2S_2$ $[M+H]^+$ 233.04184; found 233.07747.

2.2.7 2-(5-butyl-6-thioxo-1,3,5-thiadiazinan-3-yl) propionic acid (7)

Compound **7** was acquired by n-butyl amine and DL-α-alanine. Product obtained as white solid recrystallized from ethanol. Yield: 68%, mp: 98–100°C, ^1H NMR (400 MHz, DMSO-d_6): δ 0.89 (t, 3H, J = 8.0 Hz, CH_3CH_2), 1.23–1.31 (m, 2H, J = 8.0 Hz, $CH_3CH_2CH_2$), 1.35 (d, 3H, CH_3CH), 1.49–1.63 (m, 2H, $CH_2CH_2CH_2$), 3.53–3.58 (q, 1H, CH_3CH), 3.65–3.72, and 4.08–4.15 (m, 2H, NCH_2CH_2), 4.44–4.65 (m, 4H, NCH_2NCH_2S). MS (ES) 262.2, calculated: 262.39. MS (ESI) m/z (%) = 262.2 (12) $[M]^+$, 115.1 (47) $[M-147]^+$, 57.0 (100) $[C_4H_9]^+$

2.2.8 2-(5-propyl-6-thioxo-1,3,5-thiadiazinan-3-yl) acetic acid (8)

Compound **8** was acquired by propyl amine and glycine. Product obtained as white solid, recrystallized from ethanol. Yield: 64%, mp: 109–111°C. ^1H NMR (400 MHz, DMSO-d_6): δ 0.85 (t, 3H, J = 8 Hz, CH_3CH_2), 1.54–1.63 (m, 2H, $CH_3CH_2CH_2$), 3.53 (s, 2H, CH_2COOH), 3.85 (t, 2H, J = 8 Hz, NCH_2CH_2,), 4.51 (s, 2H, NCH_2S), 4.52 (s, 2H, NCH_2N), 12.69 (s, COOH); MS (ESI) m/z (%) = 234.2 (25) $[M]^+$, 147.1 (15) $[M-87]^+$, 101.1 (100) $[M-133]^+$, 42.0 (90) $[C_3H_6]^+$.

2.2.9 2-(5-butyl-6-thioxo-1,3,5-thiadiazinan-3-yl) acetic acid (9)

Compound **9** was acquired by n-butyl amine and glycine. Product obtained as white solid, recrystallized from ethanol. Yield: 62%, mp: 98–99°C. ^1H NMR (400 MHz, MEOD): δ 0.97 (t, J = 8.0 Hz, 3H, CH_2CH_3), 1.32–1.42 (m, 2H, $CH_2CH_2CH_3$), 1.61–1.69 (m, 2H, $CH_2CH_2CH_2$), 3.65 (s, 2H, CH_2COOH), 3.99 (t, 2H, J = 8 Hz, NCH_2CH_2), 4.53 (s, 2H, NCH_2S), 4.55 (s, 2H, NCH_2N). ^{13}C NMR (100 MHz, MEOD): δ 13.68 (CH_3CH_2), 20.56 ($CH_2CH_2CH_3$), 29.16 ($CH_2CH_2CH_2$), 51.55 (CH_2CH_2N), 52.47 (CH_2COOH), 59.05 (C-6), 70.53 (C-4), 172.49 (CO), 191.47 (CS). HRMS (ESI) m/z: calculated for $C_9H_{17}N_2O_2S_2$ $[M+H]^+$ 249.07314; found 249.07227.

2.2.10 2-(5-hydroxyethyl)-3-phenyl-1,3,5-thiadiazinane-2-thione (10)

Compound **10** was acquired by aniline and ethanolamine. Product obtained as white solid, recrystallized from ethanol. Yield: 61%, mp: 124–126°C. ^1H NMR (400 MHz, DMSO-d_6): δ 3.00 (t, 2H, J = 8.0 Hz, CH_2CH_2OH) 3.63 (t, 2H, J = 8 Hz, NCH_2CH_2), 4.67 (s, 2H, NCH_2S), 4.72 (s, 2H, NCH_2N), 7.23–7.47 (m, 5H, Ar–H). ^{13}C NMR (100 MHz, DMSO-d_6): δ 52.11 (NCH_2), 58.96 (CH_2OH), 59.15 (C-6), 73.61 (C-4), 127.09–129.30 (Ar–CH), 144.40 (Ar–C), 192.95 (CS). HRMS (ESI) m/z: calculated for $C_{11}H_{15}N_2OS_2$ $[M+H]^+$ 255.06; found 255.06.

2.2.11 2-(5-phenyl-6-thioxo-1,3,5-thiadiazinan-3-yl) acetic acid (11)

Compound **11** was acquired by aniline and glycine. Product obtained as white solid, recrystallized from ethanol. Yield: 59%, mp: 97–99°C. ^1H NMR (400 MHz, DMSO-d_6): δ 3.73 (s, 2H, CH_2COOH), 4.65 (s, 2H, NCH_2S), 4.71 (s, 2H, NCH_2N),

7.15–7.44 (m, 5H, Ar–H). ^{13}C NMR (100 MHz, DMSO-d_6): δ 50.99 (CH_2COOH), 58.49 (C-6), 73.39 (C-4), 127.24, 127.85, and 129.61 (Ar–CH), 144.34 (Ar–C), 170.62 (C═O), 192.95 (C═S). HRMS (ESI) m/z: calculated for $C_{11}H_{13}N_2O_2S_2$ $[M+H]^+$ 269.04184; found 269.10989.

2.2.12 2-(5-phenyl-6-thioxo-1,3,5-thiadiazinan-3-yl) propanoic acid (12)

Compound **12** was acquired by aniline and DL-α-alanine. Product obtained as white solid recrystallized from ethanol. Yield: 63%, mp: 98–100°C. ^{1}H NMR (400 MHz, DMSO-d_6): δ 1.36 (d, 3H, J = 8 Hz, CH_3CH), 3.77 (q, 1H, CH_3CH), 4.64–4.68 (m, 2H, NCH_2S) 5.23–5.36 (m, 2H, NCH_2N), 7.11–7.44 (m, 5H, Ar–H). ^{13}C NMR (100 MHz, DMSO-d_6) δ 16.55 (CH_3), 55.41(C-6), 69.84 (CH), 71.44 (C-4), 117.70, 127.48, 130.02 (Ar–CH), 144.56 (Ar–C), 174.09 (C═O), 194.02 (C═S). HRMS (ESI) m/z: calculated for $C_{12}H_{15}N_2O_2S_2$ $[M+H]^+$ 283.05749; found 283.09290.

2.2.13 2-(4-methyl-2-(5-phenyl-6-thioxo-1,3,5-thiadiazinan-3-yl) pentanoic acid (13)

Compound **13** was acquired by aniline and L-leucine. Product obtained as white solid recrystallized from ethanol. Yield: 79%, mp: 92–94°C. ^{1}H NMR (400 MHz, DMSO-d_6): δ 0.85 (dd, 6H, CH_3CH), 1.50–1.59 (m, 3H, CH_3CHCH_3, $CHCH_2CH$), 3.67–3.70 (m, 1H, $NCHCH_2$), 4.63–4.85 (m, 4H, NCH_2S, and NCH_2N), 7.21–7.44 (m, 5H, Ar–H). ^{13}C NMR (100 MHz, DMSO-d_6): δ 22.33 (CH_3CHCH_3), 23.73 (CH_3CHCH_3), 25.27 ($CHCH_2CH$), 56.66 (C-6), 61.27 (NCH), 71.32 (C-4), 127.53, 128.98, and 129.39 (Ar–CH), 144.77 (Ar–C), 173.83 (CO), 193.72 (CS). HRMS (ESI) m/z: calculated for $C_{15}H_{22}N_2O_2S_2$ $[M+2H]^+$ 326.11227; found 326.16510.

3 Biological activities

3.1 NO assay

The J774.2 (ECACC, UK) cells were obtained from Bio bank facility PCMD, ICCBS, University of Karachi. In IWAKI 75 cc flasks (Asahi Techno Glass, Japan), mouse (J774.2) macrophage cell lines (European Collection of Cell Cultures, UK) were cultured in Dulbecco's modified eagle medium (DMEM) (Sigma-Aldrich, Steinheim, Germany) with 1% streptomycin/penicillin and 10% fetal bovine serum (FBS) (N.Y. U.S.; GIBCO) and were incubated at 5% CO_2 at 37°C. Briefly, 150 µL·well^{-1} of 1×10^6 cells·mL^{-1} were added in 96-well flat bottom plates and cells were treated with *Escherichia coli* lipopolysaccharide (30 µg·mL^{-1}) (DIFCO Laboratories, Michigan, USA) and different concentrations of compounds 1, 10, and 100 (µM). The plate was incubated for 48 h at 37°C in 5% carbon dioxide. After incubation, the collected supernatant was added with Griess reagent to measure the accumulation of nitrite. The plate was read at 540 nm in spectrophotometer [40].

3.2 3-(4,5-dimethylthiazol-2-yl)-2,5-diphenyltetrazolium bromide (MTT) cytotoxicity assay

We employed the standard MTT colorimetric assay to assess the cytotoxicity of prepared compounds against the human cervical cancer HeLa cells (ATCC, Manassas, USA), which were obtained from Biobank facility PCMD and ICCBS. The cells were cultured in DMEM media supplemented with 10% FBS and 1% penicillin and streptomycin at 37°C in 5% CO_2 incubator. The 96-well flat-bottom plates were added with 6×10^4 cells·mL^{-1} and incubated for 24 h to attach cells. Next day, the media was replaced and the test compounds were added in 1, 10, and 100 (µM) concentrations in triplicates and plates were incubated at 37°C in 5% CO_2 incubator for 48 h. 50 µL of MTT (0.5 mg·mL^{-1}) was added to each well followed by further incubation of 4 h. Upon aspiration of MTT, DMSO (100 µL) was then added to wells to dissolve formazan crystals. A spectrophotometer (Molecular Devices, Spectra Max plus, CA, USA) was used to measure the reduction of MTT to formazan by reading absorbance at 540 nm. The cytotoxic activity for HeLa cells was expressed as the half maximal inhibitory concentration (IC_{50}), the concentration required to cause 50% growth inhibition.

3.3 Docking studies (methodology)

Docking studies were done using Molecular Operating Environment (2016.0802) [41]. The crystal structure of inducible nitric oxide synthase (iNOS) was taken from Protein Data Bank (PDB). 4NOS was the accession code. Preparation of three-dimensional (3-D) structures of synthesized compounds and the downloaded enzyme was carried out by using our previously reported methods [42–44]. Docking rums were carried out by using default parameters. Discovery Studio Visualizer (DS-2021) was used for the analysis of the docking results [45].

4 Results and discussion

The target 3,5-disubstituted-tetrahydro-thiadiazine-2-thiones (**1–13**) were synthesized according to Scheme 1 by the reaction of a primary amine with carbon disulfide in potassium hydroxide aqueous solution to afford their respective dithiocarbamate potassium salts, which were treated with formaldehyde followed by the addition of different amino acids and ethanolamine in phosphate buffer (pH = 7.8) to cause cyclocondensation of the dithiocarbamate intermediate. The desired products were obtained by lowering the temperature and pH of the reaction mixture.

4.1 Spectral discussion

Structures of the synthesized compounds were confirmed by spectroscopic methods including ^{1}H NMR, ^{13}C NMR, 2D-NMR, mass spectrometry, and HRMS. All the spectral results as detailed in the experimental part are in agreement with the proposed structures assigned to these compounds. Hence, the mass spectra of these compounds showed the correct molecular ions. In addition, the measured HR-MS data are in agreement with the calculated values. Furthermore, DEPT and 2D-NMR including COSY, NOESY, HSQC, and HMBC experiments showed correlations that facilitated in the ^{1}H- and ^{13}C-signal assignments to the different carbons and their attached, and/or neighboring hydrogens. All the functional analogues showed similar pattern in the chemical shifts of ^{1}H and ^{13}C NMR signals, which confirm the common molecular backbone of thiadiazine thione nucleus. ^{1}H NMR spectra of all 1,3,5-thiadiazinethiones showed singlets at 4.40–4.46 ppm, for C-4 and C-6 protons while in case of compounds **1**, **2**, and **7**, multiplet appeared in corresponding regions due to diastereotopicity being prompted by the branched substituent at N-5. Similarly, in the ^{13}C NMR spectra, the (C═S) thiocarbonyl carbon appears in 190–193 ppm range, whereas signals due to C-4 and C-6 of the thiadiazinane-2-thione nucleus appeared at 67–79 and 55–58 ppm, respectively. On the other hand, the carboxylic carbons appeared at 171–173 ppm.

4.2 Cytotoxicity

The antitumor activity of the newly synthesized compounds **1**–**13** against human cervical cancer HeLa cell line was evaluated by conducting cell viability assay using tetrazolium dye MTT. In this method, cultures of the HeLa cell line were treated with the target compounds and the results are listed in Table 1. Results show that most of the prepared compounds exhibit anticancer activity. Compounds **3**, **5**, **6**, and **9** were the most potent with IC_{50} values of <4 μM. Compound **10** was inactive whereas the rest of the series revealed significant anticancer activity with IC_{50} values in the range from 7.2 ± 0.7 to 149.7 ± 11.1 μM (Table 1). A comparison of the compounds anticancer activity against the HeLa cell line indicates that the activity of thiadiazine-2-thione nucleus was markedly affected by N-5 and N-3 substituents. The presence of the phenyl group at N-3 lowers the activity while the cyclopropyl and 3-methoxypropyl bearing moieties were found to be the most potent inhibitors. Similarly, in N-3 butyl substituted series, activity increases. On the other hand, changing the N-5 substituent from bulkier to less bulky groups increases the activity. Furthermore, results showed that activity increases with shorter chains of the acid on N5 (Figure 1).

4.3 NO activity

NO activity was assessed using J774.2 mouse macrophage cell line that was cultured in 75 cc flasks. 1, 10, and 100 μM concentration of the test compounds were added to 96-well plate incubated at 37°C in humidified air containing 5% CO_2. Nitrite accumulation in grown culture was measured by Griess reagent. All the tested compounds sowed strong NO inhibitory activities with IC_{50} values ranging from <0.4 to 14.9 μM (Table 1). Compounds **3**, **4**, **5**, **9**, and **12** bearing butyric and butanoic acid moiety at N5 exhibit IC_{50} value <0.4 (μM) while compounds **6** and **10** showed 2.15 and 14.9 μM, IC_{50} values, respectively. It was observed that among the tested series compounds bearing propionic acid at N-5 were less active as compared to butyric and butanoic acid substituted. No structure–activity relationship observed for N-3 substituents.

4.4 Docking studies

Research findings indicated that the expression of iNOS can be observed in several malignant tumors, such as lung, breast, prostate, and malignant melanoma. We carried out docking simulations on the inhibition of iNOS using the Molecular Operating Environment (MOE 2016.0802) software [44]. The 3-D crystal structure of human iNOS was

Table 1: Cytotoxic and NO inhibition of tested series

Sample codes	R1	R2	Cytotoxicity HeLa cells IC_{50} ± SD (μM)	NO inhibition IC_{50} ± SD (μM)
1	$CH_3–CH_2–CH_2–CH_2–$	CH_3-CH(CH_3)-CH_2-C(H)(COOH)-	22.0 ± 0.3	ND
2	$CH_3–CH_2–CH_2–CH_2–$	CH_3-CH_2-CH(COOH)-	13.7 ± 0.4	ND
3	$CH_3O–CH_2–CH_2–CH_2–$	$–CH_2–CH_2–COOH$	<4	<0.4
4	$CH_3O–CH_2–CH_2–CH_2–$	$–CH_2–COOH$	7.2 ± 0.7	<0.4
5	H_2C(CH-CH_2-)H_2C	CH_3-CH(COOH)-	<4	<0.4
6	H_2C(CH-CH_2-)H_2C	$–CH_2–COOH$	<4	2.15
7	$CH_3–CH_2–CH_2–CH_2–$	CH_3-CH(COOH)-	14.5 ± 3.0	ND
8	$CH_3–CH_2–CH_2–$	$–CH_2–COOH$	36.3 ± 3.8	ND
9	$CH_3–CH_2–CH_2–CH_2–$	$–CH_2–COOH$	<4	<0.4
10	$C_6H_5^-$	$–CH_2–CH_2–OH$	>400	14.9
11	$C_6H_5^-$	$–CH_2–COOH$	149.7 ± 11.1	ND
12	$C_6H_5^-$	CH_3-CH(COOH)-	38.2 ± 6.0	<0.4
13	$C_6H_5^-$	CH_3-CH(CH_3)-CH_2-C(H)(COOH)-	55.8 ± 15.1	ND
Doxorubicin			0.86 ± 0.08	
L-NMMA				97.5 ± 3.2

L-NMMA = N^G monomethyl L-arginine acetate.

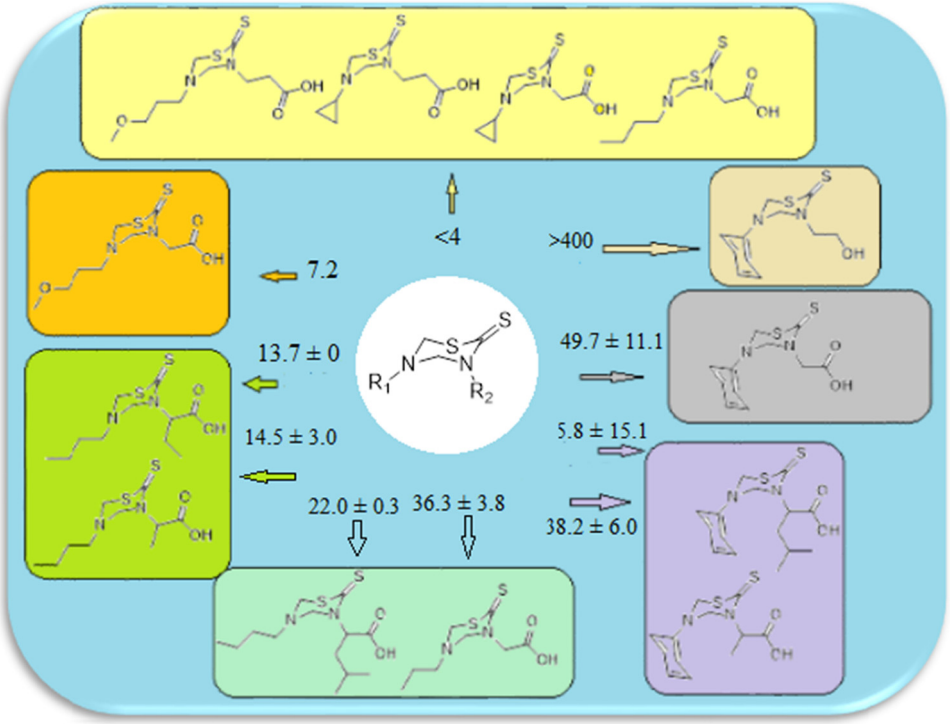

Figure 1: Structural diversity and IC_{50} – a schematic SAR.

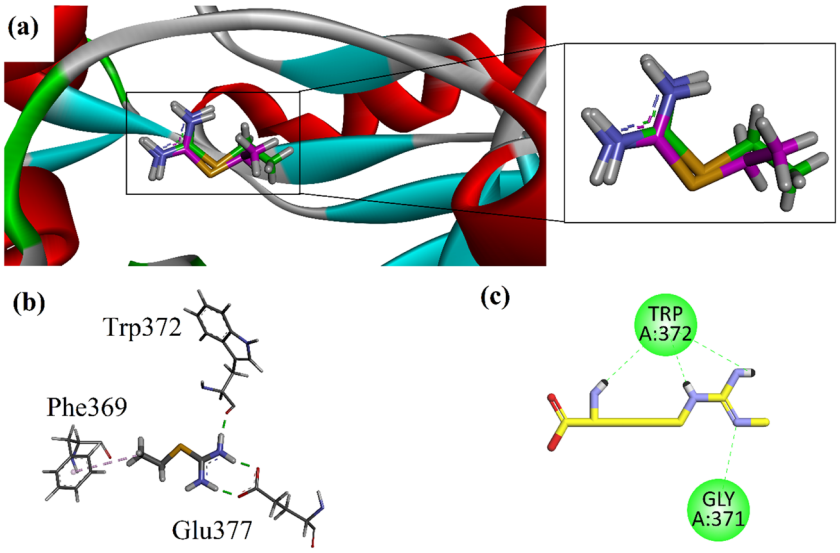

Figure 2: (a) Ribbon superposed model of native ITU (green carbon stick) and re-docked ITU (pink carbon stick); (b) 3-D interaction plots of native ITU in the binding site of iNOS (PDB ID = 4NOS); and (c) 2-D interaction plot of control drug N^G monomethyl L-arginine in the binding site of iNOS. These 3-D/2-D interactions plots are modeled by using Discovery Studio Visualizer.

acquired from PDB with accession code number 4NOS. Docking protocol was validated by using the re-dock method. Native ligand ethylisothiourea (ITU) was re-docked into the binding site. The binding orientation of the re-docked ITU and experimental ITU was analyzed. The computed root-mean square deviation was 1.13 Å, which was found within the threshold limit (<2.0 Å). The superposed results of the re-dock experiment are shown in Figure 2a. The 3-D interaction plot of native ITU showed that it interacts with Trp372 and Glu377 (Figure 2b). We also docked control drug (NO inhibitor) in the binding site of iNOS. Two-dimensional (2-D) interaction plot showed that it interacts with amino acid residues Gly371 and Trp372 *via* hydrogen bond interactions (Figure 2c).

All synthesized compounds were docked into the active site of the human iNOS (PDB ID = 3NOS). The 3-D interaction plots of studied compounds are depicted in Figures 3 and 4. The studied compounds interact with amino acid residues *via* conventional hydrogen bonds and hydrophobic interactions. Within this context,

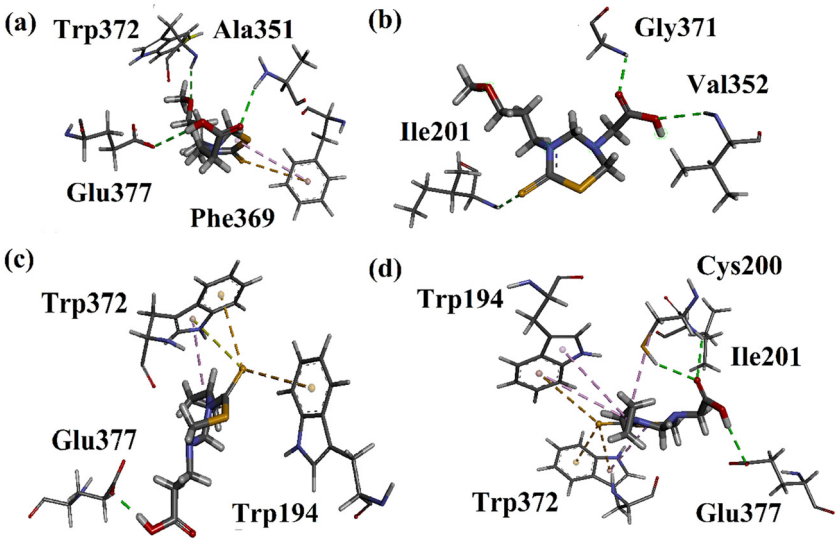

Figure 3: (a–d) 3-D interaction plots of compounds **3–6** modeled by using Discovery Studio Visualizer in the binding site of iNOS (PDB ID = 4NOS).

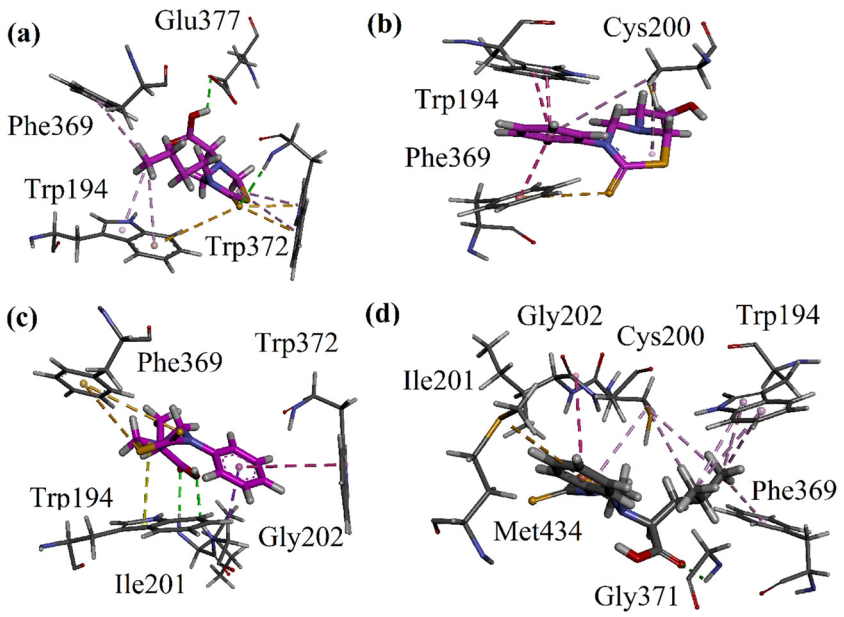

Figure 4: (a–d) 3-D interaction plots of compounds **9**, **10**, **12**, and **13** modeled by using Discovery Studio Visualizer in the binding site of iNOS (PDB ID = 4NOS).

compound **3** displayed strong hydrogen bonding interaction with Trp372, Ala351, and Glu377. In addition, a π–sulfur and π–alkyl types of interactions with Phe369 were observed (Figure 3a). Similarly, compound **4** exhibited conventional hydrogen bonding interactions with Gly371, Val352, and Ile201 (Figure 3b). On the other hand, compound **5** showed conventional hydrogen bonding interaction with Glu377 along with a bifurcated π–sulfur interaction with Trp372 (Figure 3c). In contrast, compound **6** exhibited conventional hydrogen bonding interactions with Glu377, Ile201, and Cys200 in addition to two π–sulfur interactions with Trp372 and Trp194 (Figure 3d).

Compound **9** displayed one conventional hydrogen bonding interaction with Trp32 and Glu377, and two π–sulfur interactions with Trp372 and Trp194 as shown in Figure 4a. Compound **10** showed π–π stacked interaction with Trp194 and Phe369, in addition to a π–sulfur interaction with Phe369 (Figure 4b). Similarly, compound **12** showed one conventional hydrogen bonding interaction and π–sigma interaction with Gly202, and hydrogen bond interactions with Ile201. It additionally exhibited two π–sulfur interactions with Phe369 and a π–π stacked interaction with Trp372 (Figure 4c). Similarly, compound **13** exhibited a conventional hydrogen bonding interaction with Gly371, a π–sulfur interaction with Met434, and a π–alkyl interaction with Gly202 (Figure 4d). All the binding energy values in kcal mol^{-1} and type of interactions are presented in Table 2.

Table 2: Interacting residues and binding energy of the docked compounds in the binding site of iNOS (PDB ID = 4NOS)

	Interacting residues				
Comp. no.	**Hydrogen bond**	**π–π stack**	**π–sulfur**	**π–alkyl/π–σ**	**Binding energy (kcal·mol^{-1})**
3	Trp372, Ala351, Glu377	—	Phe369	Phe369	−6.32
4	Gly371, Val352, and Ile201	—	Trp372	–	−6.04
5	Glu377	—	Trp372 (bifurcated)	—	−6.16
6	Glu377, Ile201, and Cys200	—	Trp372, Trp194	—	−6.29
9	Trp32 and Glu377	—	Trp372, Trp194	—	−6.49
10	—	Trp194 and Phe369	Phe369	—	−4.22
12	Ile201	Trp372	—	Gly202	−5.67
13	Gly371	—	Met434	—	−5.19
Control	Gly371 and Trp372	—	—	—	−4.05

5 Conclusions

In summary, we have synthesized a total of thirteen tetrahydro-2*H*-1,3,5-thiadiazine-2-thiones and have characterized by different spectroscopic methods. The prepared compounds were screened for their anticancer activity against the HeLa cell line, and NO inhibitory potential. Results revealed that most of the prepared compounds exhibit significant potential. Compounds **3**, **5**, **6**, and **9** were the most potent with IC_{50} values of <4 μM. In addition, our findings showed that all the screened compounds are strong NO inhibitors (IC_{50} values range between <0.4 and 14.9 μM). Docking studies related to iNOS showed that the studied compounds interact with the enzyme via strong hydrogen bonds and hydrophobic interactions. These findings could encourage the researchers for further insight in search of their anticancer potential or as leads in the development of anticancer drugs.

Acknowledgment: The authors are thankful to Higher Education Commission of Pakistan for providing fund for a part of this project under project no. NRPU-4165.

Funding information: This research project was funded by the Higher Education Commission under project no. NRPU-4165.

Author contributions: Haleema Ali synthesized the compounds and wrote paper under the supervision of Rasool Khan; Xiandao Pan and Farzana Shaheen did the NMR and mass analysis; Almas Jabeen did anticancer and nitric oxide activity of synthesized compounds; Abdur Rauf, Muhammad Shah, and Umer Rashid involved in docking analysis of bioactive compounds; Yahya S. Al-Awthan, Omar S. Bahattab, and Mohammed A. Al-Duais did the analysis; and Mohammad S. Mubarak involved in analysis and writing this paper. All authors read the article and approved for submission.

Conflict of interest: One of the corresponding authors (Abdur Rauf) is a member of the Editorial Board of Green Processing and Synthesis.

Data availability statement: The data associated to this work are a part of PhD thesis and can be obtain from the corresponding authors upon request.

Supporting information: The supporting information is available online (see supplementary file).

References

[1] Brisson M, Kim JJ, Canfell K, Drolet M, Gingras G, Burger EA, et al. Impact of HPV vaccination and cervical screening on cervical cancer elimination: A comparative modeling analysis in 78 low-income and lower-middle-income countries. Lancet. 2020;395(10224):575–90.

[2] Ferlay J, Colombet M, Soerjomataram I, Mathers C, Parkin DM, Piñeros M, et al. Estimating the global cancer incidence and mortality in 2018: GLOBOCAN sources and methods. Int J Cancer. 2019;144(8):1941–53.

[3] Longley D, Johnston P. Molecular mechanisms of drug resistance. J Pathol. 2005;205(2):275–92.

[4] Hausser J, Alon U. Tumour heterogeneity and the evolutionary trade-offs of cancer. Nat Rev Cancer. 2020;20(4):247–57.

[5] Wu Y, Ding Y, Ramprasath T, Zou M. Oxidative stress, GTPCH1, and endothelial nitric oxide synthase uncoupling in hypertension. A Antioxid Redox Signal. 2021;34(9):750–64.

[6] Aktan F. iNOS-mediated nitric oxide production and its regulation. Life Sci. 2004;75(6):639–53.

[7] Alderton WK, Cooper CE, Knowles RG. Nitric oxide synthases: structure, function and inhibition. Biochem J. 2001;357(3):593–615.

[8] Semeraro N, Ammollo CT, Semeraro F, Colucci M. Sepsis-associated disseminated intravascular coagulation and thromboembolic disease. Mediterr J Hematol Infect Dis. 2010;2(3):14.

[9] Bogdan C. Nitric oxide and the immune response. Nat Immunol. 2001;2(10):907–16.

[10] Aqil M, Elseth KM, Vesper BJ, Deliu Z, Aydogan B, Xue J, et al. Part I – mechanism of adaptation: high nitric oxide adapted A549 cells show enhanced DNA damage response and activation of antiapoptotic pathways. Tumour Biol. 2014;35(3):2403–15.

[11] Beevi SS, Rasheed MH, Geetha A. Evidence of oxidative and nitrosative stress in patients with cervical squamous cell carcinoma. Clinica Chim Acta. 2007;375(1–2):119–23.

[12] Hiraku Y, Tabata T, Ma N, Murata M, Ding X, Kawanishi S. Nitrative and oxidative DNA damage in cervical intraepithelial neoplasia associated with human papilloma virus infection. Cancer Sci. 2007;98(7):964–72.

[13] Altıntop MD, Sever B, Çiftçi GA, Kucukoglu K, Özdemir A, Soleimani SS, et al. Synthesis and evaluation of new benzodioxole-based dithiocarbamate derivatives as potential anticancer agents and hCA-I and HCA-II inhibitors. Eur J Med Chem. 2017;125:190–6.

[14] Alverdi V, Giovagnini L, Marzano C, Seraglia R, Bettio F, Sitran S, et al. Characterization studies and cytotoxicity assays of Pt (II) and Pd (II) dithiocarbamate complexes by means of FT-IR, NMR spectroscopy and mass spectrometry. J Inorg Biochem. 2004;98(6):1117–28.

[15] de Vos D, Ho SY, Tiekink ER. Cytotoxicity profiles for a series of triorganophosphinegold (I) dithiocarbamates and triorganophosphinegold (I) xanthates. Bioinorg Chem. 1970;2(1):1–2.

[16] Mansouri-Torshizi H, Saeidifar M, Khosravi F, Divsalar A, Saboury AA, Hassani F. DNA binding and antitumor activity of α-diimineplatinum (II) and palladium (II) dithiocarbamate complexes. Bioinorg Chem. 2011;Article ID 394506. doi: 10.1155/2011/394506.

[17] Ronconi L, Marzano C, Zanello P, Corsini M, Miolo G, Maccà C, et al. Gold (III) dithiocarbamate derivatives for the treatment of cancer: solution chemistry, DNA binding, and hemolytic properties. J Med Chem. 2006;49(5):1648–57.
[18] Crowley E, Rowan NJ, Faller D, Friel AM. Natural and synthetic isothiocyanates possess anticancer potential against liver and prostate cancer in vitro. Anticancer Res. 2019;39(7):3469–85.
[19] Citi V, Piragine E, Pagnotta E, Ugolini L, Di Cesare Mannelli L, Testai L, et al. Anticancer properties of erucin, an H2S-releasing isothiocyanate, on human pancreatic adenocarcinoma cells (AsPC-1). Phytother Res. 2019;33(3):845–55.
[20] Hać A, Brokowska J, Rintz E, Bartkowski M, Węgrzyn G, Herman-Antosiewicz A. Mechanism of selective anticancer activity of isothiocyanates relies on differences in DNA damage repair between cancer and healthy cells. Eur J Nutr. 2019;59(4):1421–32.
[21] Richa K, Karmaker R, Longkumer N, Das V, Bhuyan PJ, Pal M, et al. Synthesis, in vitro evaluation, molecular docking and DFT studies of some phenyl isothiocyanates as anticancer agents. Anti-Cancer Agents Med Chem. 2019;19(18):2211–22.
[22] Mandrich L, Caputo E. Brassicaceae-derived anticancer agents: Towards a green approach to beat cancer. Nutrients. 2020;12(3):868.
[23] Sodvadiya M, Patel H, Mishra A, Nair S. Emerging insights into anticancer chemopreventive activities of nutraceutical moringa oleifera: Molecular mechanisms, signal transduction and in vivo efficacy. Curr Pharmacol Rep. 2020;2:38–51.
[24] Arumugam A, Ibrahim MD, Kntayya SB, Mohd Ain N, Iori R, Galletti S, et al. Induction of apoptosis by gluconasturtiin-isothiocyanate (GNST-ITC) in human hepatocarcinoma HepG2 cells and human breast adenocarcinoma MCF-7 cells. Molecules. 2020;25(5):1240.
[25] El-Shorbagi AN, El-Naggar M, Tarazi H, Chaudhary S, Abdu-Allah H, Hersi F, et al. Bis-(5-substituted-2-thiono-1, 3, 5-thiadiazinan-3-yl) butane as a scaffold of anti-proliferative activity, blended by a multicomponent process. Med Chem Res. 2018;27(4):1103–10.
[26] Radwan AA, Aboul-Fadl T, Al-Dhfyan A, Abdel-Mageeda WM. Synthesis and Characterization of bis-3, 5-disubstituted thiadiazine-2-thione derivatives as anticancer agents. Asian J Chem. 2014;26(23):8145.
[27] Radwan AA, Al-Dhfyan A, Abdel-Hamid MK, Al-Badr AA, Aboul-Fadl T. 3, 5-Disubstituted thiadiazine-2-thiones: new cell-cycle inhibitors. Arch Pharm Res. 2012;35(1):35–49.
[28] Carrasco R, Padrón JA, Pérez R, Rodríguez H, Suárez M, Ochoa C. Quantitative structure antitumoral-activity relationships of thiadiazinthione derivatives using the novel hybrid molecular index. J Pharm Pharm Sci. 2005;8(3):586–92.
[29] Pérez R, Rodríguez H, Pérez E, Suárez M, Reyes O, González LJ, et al. Study on the decomposition products of thiadiazinthione and their anticancer properties. Arzneimittelforschung. 2000;50(09):854–7.
[30] Arshad N, Hashim J, Minhas MA, Aslam J, Ashraf T, Hamid SZ, et al. New series of 3, 5-disubstituted tetrahydro-2H-1, 3, 5-thiadiazine thione (THTT) derivatives: synthesis and potent antileishmanial activity. Bioorg Med Chem Lett. 2018;28(19):3251–4.
[31] Mao L, Jiang H, Wang Q, Yan D, Cao A. Efficacy of soil fumigation with dazomet for controlling ginger bacterial wilt (Ralstonia solanacearum) in China. Crop Prot. 2017;100:111–6.
[32] Coro J, Pérez R, Rodríguez H, Suárez M, Vega C, Rolón M, et al. Synthesis and antiprotozoan evaluation of new alkyl-linked bis (2-thioxo-[1, 3, 5] thiadiazinan-3-yl) carboxylic acids. Bioorg Med Chem Lett. 2005;13(10):3413–21.
[33] Coro J, Atherton R, Little S, Wharton H, Yardley V, Alvarez A, Jr, et al. Alkyl-linked bis-THTT derivatives as potent in vitro trypanocidal agents. Bioorg Med Chem Lett. 2006;16(5):1312–5.
[34] Vicentini CB, Forlani G, Manfrini M, Romagnoli C, Mares D. Development of new fungicides against Magnaporthe grisea: synthesis and biological activity of pyrazolo [3, 4-d][1, 3] thiazine, pyrazolo [1, 5-c][1, 3, 5] thiadiazine, and and pyrazolo [3, 4-d] pyrimidine derivatives. J Agric Food Chem. 2002;50(17):4839–45.
[35] Vicentini CB, Guccione S, Giurato L, Ciaccio R, Mares D, Forlani G. Pyrazole derivatives as photosynthetic electron transport inhibitors: New leads and structure– activity relationship. J Agric Food Chem. 2005;53(10):3848–55.
[36] Katiyar D, Tiwari VK, Tripathi RP, Srivastava A, Chaturvedi V, Srivastava R, et al. Synthesis and antimycobacterial activity of 3, 5-disubstituted thiadiazine thiones. Bioorg Med Chem Lett. 2003;11(20):4369–75.
[37] Semreen MH, El-Shorbagi AN, Al-Tel TH, Alsalahat IM. Targeting γ-aminobutyric acid (GABA) carriers to the brain: potential relevance as antiepileptic pro-drugs. Med Chem. 2010;6(3):144–9.
[38] Ji X, Zhong Z, Chen X, Xing R, Liu S, Wang L, Li P. Preparation of 1, 3, 5-thiadiazine-2-thione derivatives of chitosan and their potential antioxidant activity in vitro. Bioorg Med Chem Lett. 2007;17(15):4275–9.
[39] Schade W A, Rieche. Synthetische Senfölbildner, VII. Untersuchungen zum Wirkungsmechanismus der 2-Thion-tetrahydro-1,3,5-thiadiazine. Arch der Pharmazie. 1966;299(7):589–95.
[40] Grisham MB, Johnson GG, Lancaster JR, Jr. Quantitation of nitrate and nitrite in extracellular fluids, in Methods in enzymology. Academic Press. Elsevier; 1996. p. 237–46.
[41] Molecular Operating Environment (MOE), 2016.0208 Chemical Computing Group ULC, 1010 Sherbooke St. West, Suite #910, Montreal, QC, Canada, H3A 2R7; 2016.
[42] Sadiq A, MahnashimMH, Alyami BA, Alqahtani YS, Alqarni AO, Rashid U. Tailoring the substitution pattern of Pyrrolidine-2, 5-dione for discovery of new structural template for dual COX/LOX inhibition. Bioorg Chem. 2021;112:104969.
[43] Nadeem MS, Khan JA, Rashid U. Fluoxetine and sertraline based multitarget inhibitors of cholinesterases and monoamine oxidase-A/B for the treatment of Alzheimer's disease: Synthesis, pharmacology and molecular modeling studies. Int J Biol Macromol. 2021;193:19–26.
[44] Javed MA, Ashraf N, Saeed Jan M, Mahnashi MH, Alqahtani YS, Alyami BA, et al. Structural modification, in vitro, in vivo, ex vivo, and in silico exploration of pyrimidine and pyrrolidine cores for targeting enzymes associated with neuroinflammation and cholinergic deficit in Alzheimer's disease. ACS Chemical Neuroscience. 2021;12(21):4123–43.
[45] Biovia. Dassault Systèmes, Discovery Stuio Visualizer (DS-2021). San Diego: Dassault Systèmes.